Superconductive coupling in tailored [(SnSe)$_{1+\delta}$]$_m$(NbSe$_2$)$_1$ multilayers

Martina Trahms[1,4] , **Corinna Grosse**[1,5], **Matti B Alemayehu**[2], **Omar K Hite**[2], **Olivio Chiatti**[1], **Anna Mogilatenko**[1,3], **David C Johnson**[2] and **Saskia F Fischer**[1]

[1] Novel Materials Group, Humboldt-Universität zu Berlin, Newtonstr. 15, 12489 Berlin, Germany
[2] Department of Chemistry and Materials Science Institute, University of Oregon, Eugene, OR 97403, United States of America
[3] Ferdinand-Braun-Institut, Leibniz-Institut für Höchstfrequenztechnik, 12489 Berlin, Germany

E-mail: sfischer@physik.hu-berlin.de

Abstract

Ferecrystals are a new artificially layered material system, in which the individual layers are stacked with monolayer precision and are turbostratically disordered. Here, the superconducting coupling of the NbSe$_2$ layers in [(SnSe)$_{1+\delta}$]$_m$[NbSe$_2$]$_1$ ferecrystals with m between 1 and 6 are investigated. The variation of m effectively increases the distance between the superconducting NbSe$_2$ monolayers. We find a systematic decrease of the transition temperature with an increasing number of SnSe layers per repeat unit. For $m = 9$ a superconducting transition can no longer be observed at temperatures above 250 mK. In order to investigate the superconducting coupling between individual NbSe$_2$ layers, the cross-plane Ginzburg–Landau coherence lengths were determined. Electric transport measurements of the superconducting transition were performed in the presence of a magnetic field, oriented parallel and perpendicular to the layers, at temperatures closely below the transition temperature. A decoupling with increasing distance of the NbSe$_2$ layers is observed. However, ferecrystals with NbSe$_2$ layers separated by up to six layers of SnSe are still considered as three-dimensional superconductors.

Keywords: superconducting thin films, Ginzburg–Landau coherence lengths, superconductor–semiconductor hybrid layers, transition temperatures, coupling

(Some figures may appear in colour only in the online journal)

1. Introduction

The investigation of two-dimensional (2D) phenomena in thin layers of various materials has received much attention lately [1–4]. As the thickness of the layers decreases down to atomic dimensions, novel physical phenomena can be observed. A well investigated example is graphene, which changes its physical properties dramatically upon the transition from three-dimensional (3D) crystal (graphite) to a 2D atomic layer [4].

Transition metal dichalcogenides (TMDCs) are another group of materials that is interesting for the investigation of 2D phenomena [5]. TMDCs are layered materials with layers that are weakly bound by van der Waals forces, which permits the exfoliation of these materials down to a few atomic layers [2]. The materials that belong to the group of TMDCs exhibit a wide range of electrical properties, varying from insulating over metallic to superconducting. This makes them well suited for the investigation of 2D phenomena and for the development of new technologies [6]. Deterioration of these thin, layered materials is one of the main issues when it comes to the investigation of their physical properties. The advantages of the so-called buried layers, i.e. thin layers that are embedded in a matrix of other materials, are their stability
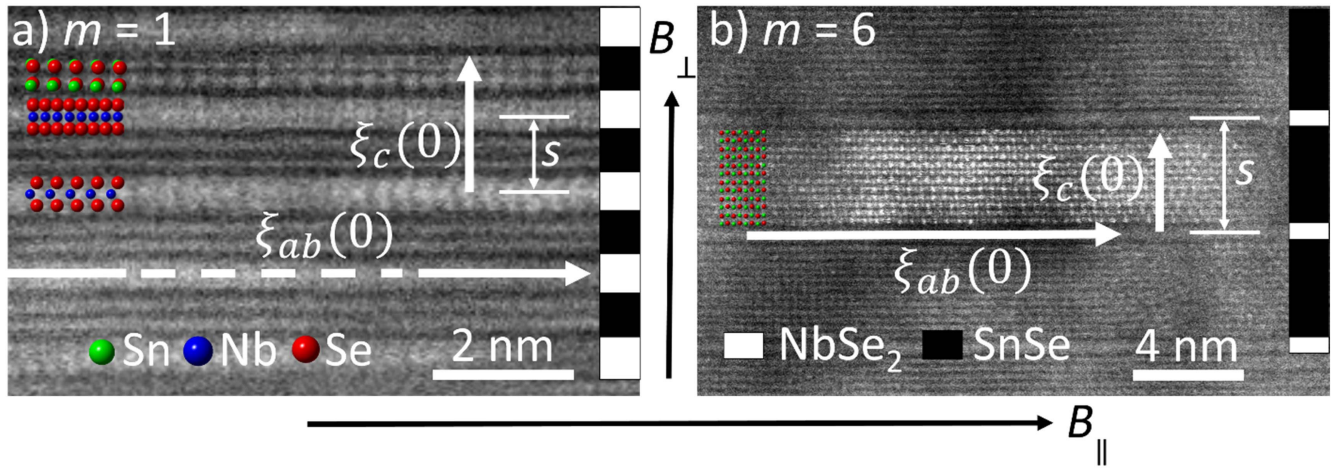
Figure 1. Transmission electron microscopy images of two of the investigated [(SnSe)$_{1+\delta}$]$_m$[NbSe$_2$]$_1$ ferecrystals with (a) $m = 1$ and (b) $m = 6$, showing the monolayer precision of the deposition technique [16]. The distance between NbSe$_2$ monolayers s and the determined cross-plane $\xi_c(0)$ and in-plane coherence length $\xi_{ab}(0)$ are shown as an illustration. The dashed line in (a) indicates that this coherence length is not to scale in the image. The orientation of the magnetic fields with respect to the layered structure is also indicated.

against environmental influences and a higher flexibility for the design of new technologies.

Ferecrystals are material systems consisting of at least two materials that are stacked in a periodically repeating sequence. The layering sequences of these materials can be controlled on the atomic scale. In contrast to the so-called misfit layer compounds (MLCs) [7, 8], ferecrystals have a much weaker lattice adjustment between layers due to their turbostratic disorder. Turbostratic disorder describes the rotation of the individual layers around the c-axis by an arbitrary angle [9–11]. This property allows for a wide range of possible stacking sequences and materials that can be realized as ferecrystals.

In this work ferecrystals consisting of the TMDC NbSe2 and the semiconductor SnSe are investigated. NbSe$_2$ as a bulk material is a metal that becomes superconducting below a critical temperature of $T_c = 7.3$ K [12]. The exfoliation of NbSe2 down to a single monolayer was recently accomplished by Xi *et al* [2]. In this case the transition temperature was reduced to $T_{c,\text{layer}} = 3.1$ K. As ferecrystals can be produced with atomic precision, it is possible to observe the influence of a systematically increasing the distance between single NbSe$_2$ layers on the superconducting properties of the system. The separation of NbSe$_2$ monolayers is controlled by the exact number of monolayers of SnSe that are incorporated per repeat unit. This makes them an ideal system for the investigation of the coupling between superconducting layers, by increasing their distance, so that the 3D system begins to cross-over to two dimensions.

In our previous studies a structural and electrical analysis of various types of ferecrystals is provided in comparison to their counterparts realized as MLCs [9]. The in-plane structures of ferecrystals composed of a number of various materials and layering sequences are investigated in [13]. A detailed description of the structural and electrical properties of [(SnSe)$_{1+\delta}$]$_m$[NbSe$_2$]$_n$ ferecrystals can be found in [11, 14–17]. The structural details and electrical characterization

of these particular compounds above a temperature of 15 K with $n = 1$ were presented by Alemayehu *et al* [14]. Superconductivity in these ferecrystals was shown along with a detailed structural analysis. It has also been shown that a systematic decrease of the transition temperature can be observed with increasing separation between superconducting layers [16]. This can have several explanations, including the decoupling of the individual superconducting layers.

In this work, we investigate the coupling strength between the superconducting layers in ferecrystals with $m = 1, 3, 5$, and 6 SnSe layers per repeat unit. In these highly anisotropic thin films the parallel as well as perpendicular Ginzburg–Landau (GL) coherence lengths were determined by performing measurements of the superconducting transition in the presence of an external magnetic field, oriented parallel and perpendicular to the layers of the system. The cross-plane GL coherence length indicates whether the anisotropic GL model (strong inter-layer coupling) or the Lawrence–Doniach model (weak inter-layer coupling) is more appropriate for these ferecrystals [20].

2. Methods

The synthesis of the ferecrystals is explained in detail elsewhere [15, 16]. The structure of ferecrystals can be tailored with monolayer precision in a physical vapor deposition process with a subsequent annealing step. In figure 1 a high-angle annular dark-field scanning transmission electron microscopy image of the investigated ferecrystals with $m = 1$ and $m = 6$ is shown, confirming that monolayer precision is achieved in these ferecrystals [11, 16]. The turbostratic disorder as well as different grains can also be observed in these images [16].

Electrical transport measurements were performed on ferecrystals that were deposited through a shadow mask in a cross and cloverleaf form. These geometries are very well

suited to perform four-point van der Pauw (vdP) measurements. Thin gold wires were attached at each leaf by small indium pieces and the substrates were subsequently glued to a chip carrier using silver paste.

Low temperatures down to 250 mK were achieved within an Oxford Instruments Heliox ^{3}He cryostat. A superconducting magnet with magnetic fields up to 10 T was used to perform magnetic field dependent resistance measurements. In order to align the sample parallel or perpendicular to the magnetic field two different kinds of sample holder systems were used. One consists of static holders that can be mounted to the ^{3}He system before cooling, aligning the sample either parallel or perpendicular to the magnetic field direction. This method provides a very good thermal contact between the sample, ^{3}He bath, and thermometer, while the alignment with the magnetic field cannot be adjusted during operation. The other stage includes the possibility to rotate the sample during operation (used for the parallel critical field determination of $m = 3$ and $m = 5$). This system allows a more precise alignment, which is especially crucial for the parallel alignment of the magnetic field with the layers of the ferecrystals. However, the thermal contact to the ^{3}He bath and the temperature sensor suffers from the more complex rotating system. The low-temperature measurements below 2.5 K were performed using a calibrated RuOx thermometer located close to the sample holder.

The magnetic fields were generated by a superconducting coil with magnetic fields up to 10 T. Generally, the magnetic field was swept in a quasi-static way, keeping the magnetic field constant for several minutes before collecting the data. The reason for this procedure was a large difference in the measured resistances between upwards and downwards sweeps of the magnetic field when sweeping the field continuously. This time-dependent hysteresis was especially pronounced in the parallel field configuration and for ferecrystals with high m values. The only data set that was measured in a continuously swept magnetic field, was the $m = 1$ ferecrystal in the presence of a perpendicular magnetic field as the observed time-dependent hysteresis was very weak.

Two kinds of resistance measurements were performed on the ferecrystals. In order to extract the sheet resistance the vdP method was applied. I–V-curves were measured in all four possible vdP configurations and the sheet resistance was calculated according to [18, 19]. On the other hand, a four-point measurement in only one of the vdP configurations was performed using a lock-in amplifier (DSP 7265, SR 830). In general, an AC current of 50 nA was applied to two of the contacts using a high resistance of 1 MΩ at the voltage output of the lock-in amplifier and the voltage at the other two contacts was measured. Reference measurements at 15 nA did not lead to differences in the temperature- or magnetic-field-dependent superconducting transition, indicating that the current chosen is far enough below the critical current value of the material.
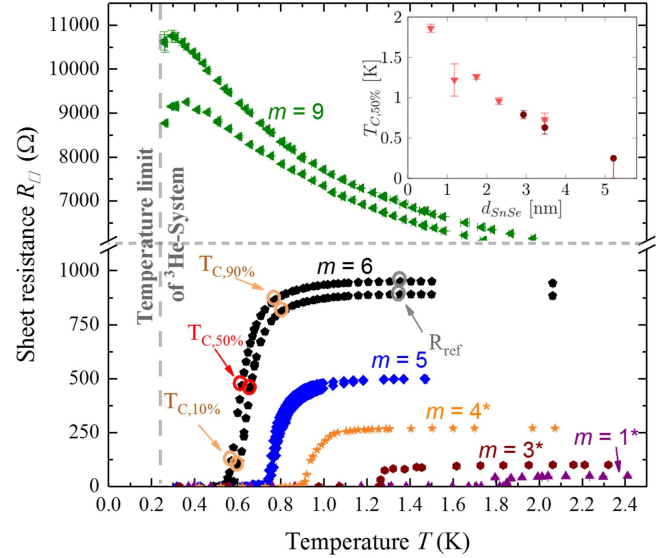

Figure 2. Temperature-dependent resistance for different ferecrystals with $m = 1, 3, 4, 6,$ and 9 measured for two different sample geometries. The inset shows the transition temperature dependence on the separation of adjacent NbSe$_2$ layers. Data from our previous work [16] is marked with an *.

3. Results

Recording the resistance of the ferecrystals as a function of temperature, see figure 2, reveals that the superconducting transition takes place for all ferecrystals between $m = 1$ and $m = 6$, as has been shown in [16]. The ferecrystal with $m = 9$ layers of SnSe separating the NbSe$_2$ layers does not show a complete superconducting transition above 250 mK. However, an onset of that transition is visible. In order to determine comparable values for the transition temperature, a reference sheet resistance value R_{ref} well above the transition temperature was chosen for each sample and the critical temperature $T_{c,50\%}$ was determined at the point where the sheet resistance reduces to 50% of that value. A lower and upper limit for the transition temperature can be set at 10% and 90% of R_{ref}. The transition is shifted towards lower temperatures as the number of SnSe layers per repeat unit is increased (see the inset of figure 2). Additionally, it can be observed that the magnitude of the sheet resistance per layer increases strongly with increasing m, e.g. from 3 kΩ ($m = 1$) to 15 kΩ ($m = 9$). It is also noted that the resistance of the $m = 9$ sample increases strongly before it sets on for the superconducting transition. For the other ferecrystals with $m \geqslant 3$ it can also be observed that the resistance starts to increase at low temperatures, however, the effect is less pronounced for these samples [16].

For the ferecrystals with $m = 1, 3, 5,$ and 6 the magnetic field dependences of the resistance were recorded in the presence of a parallel and perpendicular magnetic field at constant temperatures below T_c (figure 3). As for the critical temperature, it is not trivial to determine the critical field value, due to the broadness of the transition. Here, the analysis was done using several critical field values within the
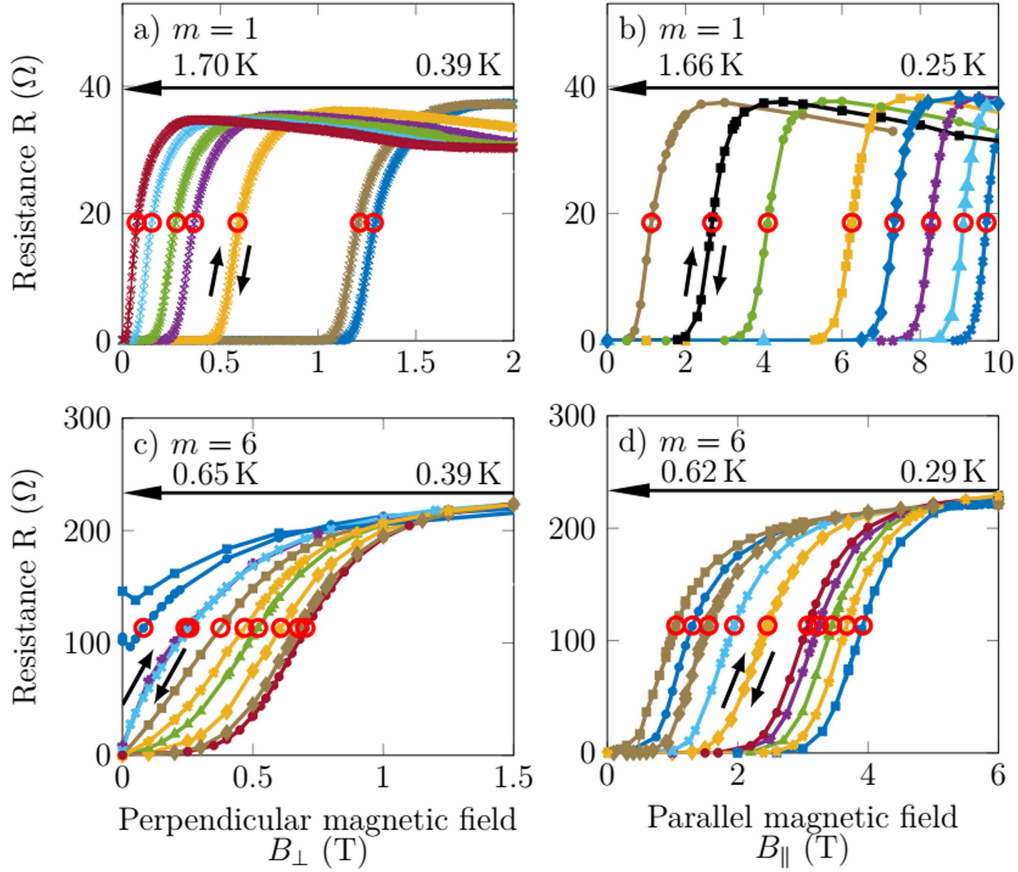
Figure 3. Resistance versus perpendicular and parallel magnetic field for $[(SnSe)_{1.16}]_m(NbSe_2)_1$ with $m = 1$ shown in (a) and (b) and $m = 6$ in (c) and (d). B_c values were defined as the magnetic field at 50% of a reference resistance value above T_c.
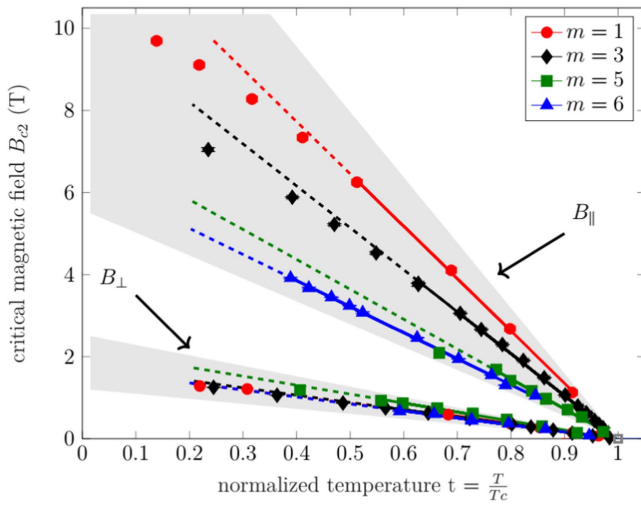
Figure 4. Critical perpendicular magnetic field $B_{c\perp}(T)$ and critical parallel magnetic field $B_{c\parallel}(T)$ for $[(SnSe)_{1.16}]_m(NbSe_2)_1$ with $m = 1$, 3, 5, and 6. The fits were done according to the Lawrence–Doniach model (equations (3.1) and (3.2)).

transition between 10% and 90% of a reference resistance value for the subsequent fit, to determine a mean value of the GL coherence lengths. From the temperature dependence of the parallel and perpendicular critical magnetic fields the perpendicular and parallel GL coherence length can be

calculated using the GL and Lawrence–Doniach models, respectively.

In the GL theory the dependence of the critical magnetic field on the temperature-dependent GL coherence length is given in [20, 21]. In highly anisotropic materials the GL coherence length can vary for the different orientations within the material. Due to the layered structure of the ferecrystals, the parallel GL coherence length ξ_{ab} can be assumed isotropic within the plane parallel to the layers. In the presence of a perpendicular critical magnetic field the superconducting properties depend only on ξ_{ab} [20–24]:

$$B_{c\perp} = \frac{\Phi_0}{2\pi\xi_{ab}(T)^2} = \frac{\Phi_0}{2\pi\xi_{ab}(0)^2}\left(1 - \frac{T}{T_c}\right), \qquad (3.1)$$

with the flux quantum $\Phi_0 = 2.07 \cdot 10^{-15}\,\mathrm{Tm}^2$ and the temperature-dependent GL coherence length

$$\xi(T) = \xi(0) \cdot \left(1 - \frac{T}{T_c}\right)^{-\frac{1}{2}}.$$

In a parallel magnetic field, the temperature dependence of the critical field values can be described by the Lawrence–Doniach model in the anisotropic GL limit near the T_c for fully coupled layers (3D):

$$B_{c\parallel} = \frac{\Phi_0}{2\pi\xi_{ab}(T)\xi_c(T)} = \frac{\Phi_0}{2\pi\xi_{ab}(0)\xi_c(0)}\left(1 - \frac{T}{T_c}\right). \quad (3.2)$$

Table 1. In-plane and cross-plane coherence lengths $\xi_{ab}(0)$ and $\xi_c(0)$ and $\xi_c(0)/(s/\sqrt{2})$, where s is the distance between two consecutive superconducting layers. $\xi_c(0)/(s/\sqrt{2}) < 1$ would indicate the transition from a bulk superconductor to individual weakly coupled 2D layers.

m	In-plane coherence length $\xi_{ab}(0)$ (nm)	Cross-plane coherence length $\xi_c(0)$ (nm)	Repeat unit distance s (nm)	Ratio $\xi_c(0)/\dfrac{s}{\sqrt{2}}$
Single crystal [25–28]	9.0–11.0	2.7–4.0	0.60	≈ 8
1	13.3 ± 0.8	1.9 ± 0.1	1.223 ± 0.001	2.2 ± 0.1
3	13.8 ± 0.5	2.4 ± 0.1	2.378 ± 0.001	1.4 ± 0.1
5	12.3 ± 0.5	3.7 ± 0.5	3.533 ± 0.001	1.5 ± 0.2
6	14 ± 1	3.7 ± 0.6	4.106 ± 0.001	1.3 ± 0.2

The respective coherence lengths and magnetic field directions are indicated in figure 1.

Both equations (3.1) and (3.2) suggest a linear dependence of the parallel and perpendicular critical fields on temperatures near the transition temperature. This dependence can be observed in figure 4, where the parallel and perpendicular critical fields (taken at 50% of the reference value) are shown in dependence on the temperature. The linear dependence close to the critical temperature can be explored to calculate both coherence lengths of the anisotropic ferecrystals. For lower temperatures the data deviates from the linear behavior as expected. The resulting coherence lengths are shown in table 1 in comparison to the distance s between two consecutive superconducting layers. The distance s was determined by x-ray diffraction [14] and confirmed by scanning transmission electron microscopy and selected-area electron diffraction [16].

4. Discussion

A criterion for 2D layers with weak Josephson coupling between the layers [20] can be formulated as

$$\xi_c(0) < \frac{s}{\sqrt{2}}. \tag{4.1}$$

Therefore, the ratio between the cross-plane GL coherence lengths and the distance between the superconducting layers, $\xi_c(0)/(s/\sqrt{2})$, is further on taken as a measure for the coupling strength between two adjacent superconducting NbSe$_2$ layers. Table 1 clearly shows that the coherence length $\xi_c(0)$ increases with the distance s for ferecrystals with $m > 1$. A similar behavior was observed for other thin layered superconductors [24]. From the criterion stated in equation (4.1) and the ratio $\xi_c(0)/(s/\sqrt{2}) > 1$ we conclude that the investigated ferecrystals, from $m = 1$–6, all show 3D superconductivity. However, a decrease in the coupling strength is clearly observed as the ratio $\xi_c(0)/(s/\sqrt{2})$ decreases by about 40% from 2.1 ± 0.1 for $m = 1$–1.3 ± 0.2 for $m = 6$. This may indicate that fully decoupled layers with $\xi_c(0)/(s/\sqrt{2}) < 1$ could possibly be achieved by further separating the superconducting layers, i.e. by increasing m beyond 6. It is also likely that a higher bandgap material or even an insulating material might be better suited for separating the superconducting layers and to reduce the coupling between adjacent layers.

The in-plane coherence lengths are almost all within error of one another and show no particular dependence on m. This indicates that the in-plane properties with respect to the superconductivity in the ferecrystals do not vary significantly between ferecrystals with different stacking sequences. Note that the in-plane coherence length is higher than that of bulk single crystals of NbSe$_2$ [28]. As the in-plane coherence length for $T < T_c$ depicts an increased average size of the normal-conducting regions due to thermal fluctuations [20], an increase of the in-plane coherence length for NbSe$_2$ monolayers in ferecrystals with respect to that for bulk NbSe$_2$ is consistent with the proximity effect due the adjacent normal-conducting SnSe layers in the ferecrystals.

The proximity effect is also consistent with the decreasing critical temperature with increasing thickness of the SnSe layers [20], i.e. with increasing m, as can be seen in figure 2. However, a reduced critical temperature may have other causes as well. The band structure of the individual layers might be influenced by the closely packed layering scheme. This can result in a charge transfer between adjacent layers, which leads to a decreasing density of states at the Fermi level in the superconducting layers [16]. Disorder within the superconducting layers might be a possible reason for the decreasing T_c [29]. Disorder is also consistent with the fact that the sheet resistance per NbSe$_2$ layer increases dramatically with m. The cross-plane GL coherence lengths indicate that the superconducting coupling between NbSe$_2$ layers decreases with increasing m is also a possible cause for the reduction of the transition temperature.

5. Conclusion

The superconducting properties of $[(SnSe)_{1+\delta}]_m[NbSe_2]_1$ ferecrystals with m between 1 and 6 were investigated as a new artificially layered superconducting material. As the number of SnSe layers m separating single NbSe$_2$ layers systematically increases, it is observed that the transition temperature decreases from above 1.8 K ($m = 1$) to about 0.6 K ($m = 6$). This may have its origin in a decreasing coupling between adjacent NbSe$_2$ layers. The decreasing coupling was indicated by the cross-plane GL coherence lengths which scales with the distance between the superconducting layers, i.e. they increase from $\xi_c(0) = (1.9 \pm 0.1)$ nm to (3.7 ± 0.6) nm with increasing separation of the NbSe$_2$ layers from $s = (1.25 \pm 0.05)$ nm to (4.14 ± 0.07) nm for $m = 1$–6, while the in-plane GL

coherence length $\xi_{ab}(0)$ remains constant at about 13–14 nm. According to the criterion derived from the Lawrence–Doniach model, the investigated ferecrystals are therefore considered as 3D superconductors $(\xi_c(0)/(s/\sqrt{2}) > 1)$. However, a complete decoupling $(\xi_c(0)/(s/\sqrt{2}) < 1)$ and the transition to 2D superconductivity may be achieved by further separating the superconducting layers with $m > 6$ or using a higher bandgap material to separate the superconducting layers.

Acknowledgments

ORCID iDs

Martina Trahms ● https://orcid.org/0000-0001-9903-8268
Saskia F Fischer ● https://orcid.org/0000-0002-1088-3615

References

[1] Wang Q H, Kalantar-Zadeh K, Kis A, Coleman J N and Strano M S 2012 Electronics and optoelectronics of two-dimensional transition metal dichalcogenides *Nat. Nanotechnol.* **7** 699

[2] Xi X *et al* 2015 Strongly enhanced charge-density-wave order in monolayer $NbSe_2$ *Nat. Nanotechnol.* **10** 765–9

[3] Ugeda M M *et al* 2016 Characterization of collective ground states in single-layer $NbSe_2$ *Nat. Phys.* **12** 92–U126

[4] Geim A K and Novoselov K S 2007 The rise of graphene *Nat. Mater.* **6** 183

[5] Geim A K and Grigorieva I V 2013 Van der Waals heterostructures *Nature* **499** 419

[6] Chhowalla M, Shin H S, Eda G, Li L-J, Loh K P and Zhang H 2013 The chemistry of two-dimensional layered transition metal dichalcogenide nanosheets *Nat. Chem.* **5** 263–75

[7] Nader A, Briggs A, Meerschaut A and Lafond A 1997 Superconductivity in the misfit layer compound $(PbSe)_{1.12}(NbSe_2)_2$ *Solid State Commun.* **102** 401–3

[8] Wiegers G A 1996 Misfit layer compounds: structures and physical properties *Prog. Solid State Chem.* **24** 1–139

[9] Beekman M, Heideman C L and Johnson D C 2014 Ferecrystals: non-epitaxial layered intergrowths *Semicond. Sci. Technol.* **29** 064012

[10] Merrill D R, Moore D B, Bauers S R, Falmbigl M and Johnson D C 2015 Misfit layer compounds and ferecrystals: model systems for thermoelectric nanocomposites *Materials* **8** 2000–29

[11] Alemayehu M B, Falmbigl M, Grosse C, Ta K, Fischer S F and Johnson D C 2015 Structural and electrical properties of a new $([SnSe]_{(1.16)})_{(1)}(NbSe_2)_{(1)}$ polytype *J. Alloys Compd.* **619** 861–8

[12] Soto F *et al* 2007 Electric and magnetic characterization of $NbSe_2$ single crystals: anisotropic superconducting fluctuations above TC *Physica* C **460–462** 789–90

[13] Falmbigl M, Alemayehu M B, Merrill D R, Beekman M and Johnson D C 2015 In-plane structure of ferecrystalline compounds *Cryst. Res. Technol.* **50** 464–72

[14] Alemayehu M B *et al* 2015 Structural and electrical properties of $([SnSe]_{(1+delta)})_{(m)}(NbSe_2)_{(1)}$ compounds: single $NbSe_2$ layers separated by increasing thickness of SnSe *Chem. Mater.* **27** 867–75

[15] Alemayehu M B, Falmbigl M, Ta K and Johnson D C 2015 Effect of local structure of $NbSe_2$ on the transport properties of $([SnSe]_{(1.16)})_{(1)}(NbSe_2)_{(n)}$ ferecrystals *Chem. Mater.* **27** 2158–64

[16] Grosse C, Alemayehu M B, Mogilatenko A, Chiatti O, Johnson D C and Fischer S F 2017 Superconducting tin selenide/niobium diselenide ferecrystals *Cryst. Res. Technol.* **52** 1700126

[17] Grosse C *et al* 2016 Superconducting ferecrystals: turbostratically disordered atomic-scale layered $(PbSe)_{(1.14)}(NbSe_2)_{(n)}$ thin films *Sci. Rep.* **6** 33457

[18] van der Pauw L J 1958 A method of measuring specific resistivity and Hall coefficients of lamallae of arbitrary shape *Philips Tech. Rev.* **20** 220–4

[19] van der Pauw L J 1958 A method of measuring specific resistivity and Hall effect of discs of arbitrary shape *Philips Tech. Rev.* **13** 1–9

[20] Klemm R A 2012 *Layered Superconductors* (Oxford: Oxford University Press)

[21] Buckel W and Kleiner R 2013 *Supraleitung* 7th edn (Weinheim: Wiley-VCH)

[22] Tinkham M 2004 *Introduction to Superconductivity* (New York: Dover)

[23] Harper F E and Tinkham M 1968 The mixed state in superconducting thin films *Phys. Rev.* **172** 441–50

[24] Inoue H, Kim M, Bell C, Hikita Y, Raghu S and Hwang H Y 2013 Tunable coupling of two-dimensional superconductors in bilayer $SrTiO_3$ heterostructures *Phys. Rev.* B **88** 241104

[25] Garoche P, Veyssie J, Manuel P and Molinie P 1976 Experimental investigation of superconductivity in 2h-NbSe$_2$ single-crystal *Solid State Commun.* **19** 455–60

[26] Foner S and Mcniff E 1973 Upper critical fields of layered superconducting $NbSe_2$ at low-temperatures *Phys. Lett.* A **45** 429–30

[27] Molinie P, Jerome D and Grant A 1974 Pressure-enhanced superconductivity and superlattice structures in transition-metal dichalcogenide layer crystals *Phil. Mag.* **30** 1091–103

[28] Sanchez D, Junod A, Muller J, Berger H and Lévy F 1995 Specific heat of 2H-$NbSe_2$ in high magnetic fields *Physica* B **204** 167–75

[29] Baturina T I, Islamov D R, Bentner J, Strunk C, Baklanov M R and Satta A 2004 Superconductivity on the localization threshold and magnetic-field-tuned superconductor–insulator transition in TiN films *JETP Lett.* **79** 337–41